21st Australasian Fluid Mechanics Conference
Adelaide, Australia
10-13 December 2018

Stochastic Subgrid Turbulence Parameterisation of Eddy-Eddy, Eddy-Meanfield, Eddy-Topographic and Meanfield-Meanfield Interactions in the Atmosphere

V. Kitsios[1] and J. S. Frederiksen[2]

[1]CSIRO Oceans and Atmosphere, Hobart, Tasmania 7000, Australia

[2]CSIRO Oceans and Atmosphere, Aspendale, Victoria 3195, Australia

Abstract

Stochastic subgrid turbulence parameterisations are developed for a baroclinic quasi-geostropic (QG) atmosphere with a January background state and realistic topography. The parameterisation coefficients are calculated from the statistics of higher resolution reference direct numerical simulations (DNS). Separate parameterisations are developed for each of the fundamental subgrid interactions. The first are the transient eddy-eddy interactions, which are between subgrid and resolved eddies. The second are the eddy-meanfield interactions between the subgrid eddies and the resolved meanfield. The third are the meanfield-meanfield interactions between the resolved meanfield and topography and their unresolved counterparts. Finally the eddy-topographic interactions are between the subgrid eddies and the resolved topography. This parameterisation framework is validated by producing large eddy simulations (LES) of the atmosphere that agree with the reference DNS. As compared to the DNS of truncation wavenumber 63, successful LES are produced with a truncation wavenumber of 15, using only 1.3% of the computational effort. This is particularly impressive as it captures both the drain of energy out of the system due to the forward enstrophy cascade, and the injection of energy associated with the unresolved baroclinic instability.

Introduction

There is the ever-growing need for larger ensemble sizes of circulation models whether it be for data assimilation, ensemble prediction, or parameter sensitivity studies. This significantly increases the computational resources. There is, therefore, a need to run lower resolution LES that represent the dynamics captured in higher resolution models. In LES the large scales are explicitly resolved on a computational grid, with the unresolved subgrid interactions parameterised. Subgrid parameterisations are typically developed by prescribing a physically inspired functional form, which is then implemented into a solver, with its performance evaluated for various benchmark flows. In the framework adopted herein, minimal assumptions are made concerning the nature of subgrid turbulence with the parameterisation coefficients determined from the statistics of judiciously truncated high resolution DNS. Physical interpretations and possible simplifications, are made after the fact from the properties of the coefficients. The only assumption made is that the subgrid interactions are quasi-diagonal in scale space [2].

As in general, it is only possible to represent the statistical effects of the unresolved nonlinear subgrid interactions, statistical dynamical closure theory is the natural formulation for developing subgrid parameterisations. Refer to [2] for an historical account of the relevant closure research. Specifically the quasi-diagonal direct interaction approximation (QDIA) closure accounts for cross correlations between field variables, but has the remarkable property that the operators and stochastic backscatter variance are diagonal in spectral space [2, 3]. Within this framework there are four classes of subgrid interactions: eddy-eddy (E-E); eddy-meanfield (E-M); meanfield-meanfield (M-M); and eddy-topographic (E-T). General expressions representing each of these subgrid interaction types were derived in [2] for inhomogeneous turbulence. These expressions were calculated for barotropic atmospheric flows in [9].

To broaden the applicability of the QDIA, a stochastic modelling approach was developed in [5] that determines the E-E subgrid coefficients from the statistics of a higher resolution reference DNS. The DNS is truncated back to a coarser grid and the parameterisation coefficients are then determined from the subgrid statistics. This approach has produced lower resolution LES that reproduces the statistics of DNS, for atmospheric, oceanic and three-dimensional wall bounded turbulent flows [10, 11, 6, 7, 8]. In addition, for truncations made within a self-similar inertial range, the subgrid coefficients are governed by simple resolution dependent scaling laws [6, 7]. These scaling laws enable the subgrid models to be utilised more widely as they remove the need to generate associated coefficients from a reference simulation.

In the current study we develop parameterisations of the key subgrid interactions for simulations of a two-level QG atmospheric flow, with a fully three-dimensional time averaged climate. We use the stochastic subgrid modelling approach of [5] to calculate the E-E parameterisation coefficients, and a new regression method to decompose the mean subgrid tendency into the E-M, E-T, and M-M components. The method is validated by comparing LES adopting these subgrid coefficients with the DNS on the basis of kinetic energy spectra and mean zonal jets.

Benchmark direct numerical simulation

We employ the two-level quasi-geostrophic model of [1], non-dimensionalised by using the radius of the earth ($a = 6371$km) as a length scale, and the inverse of the earth's angular velocity ($\Omega = 7.292\times10^{-5}$s^{-1}) as a time scale. It is spectrally discretised in the horizontal by expanding the field variables in spherical harmonics with the zonal (longitudinal) wavenumber, m, and the total wavenumber, n. This leads to the prognostic equations for the reduced potential vorticity spectral coefficients, $q^j_{mn} = \zeta^j_{mn} + (-1)^j F_L(\psi^1_{mn} - \psi^2_{mn})$, where the superscript l on the flow variables denotes the level, with $j = 1$ represents the upper level at 250hPa, and $j = 2$ the lower level at 750hPa. $\zeta^j_{mn} = -n(n+1)\psi^j_{mn}$ are the spectral coefficients of the vorticity, and ψ^j_{mn} the streamfunction coefficients. The layer coupling parameter, F_L, is inversely proportional to the temperature difference between the two levels. The evolution equation for q^j_{mn} is

$$\frac{\partial q^j_{mn}}{\partial t} = \sum_{(p,q,r,s)\in\mathbf{T}} \mathrm{i}K^{mpr}_{nqs}\left(\psi^j_{-pq}q^j_{-rs} + \psi^j_{-pq}h_{-rs}\delta^{j2}\right) - \mathrm{i}\omega_{mn}\zeta^j_{mn} - \alpha^j_n\zeta^j_{mn} + \kappa_n(\tilde{q}^j_{mn} - q^j_{mn}) - D^l_0(n)q^j_{mn}\,, \quad (1)$$

where the triangular truncated wavenumber set

$$\mathbf{T}(T) = [\ p,q,r,s\ |\ -T \le p \le T\ ,\ |p| \le q \le T\ , \quad -T \le r \le T\ ,\ |r| \le s \le T\ ]\,, \quad (2)$$

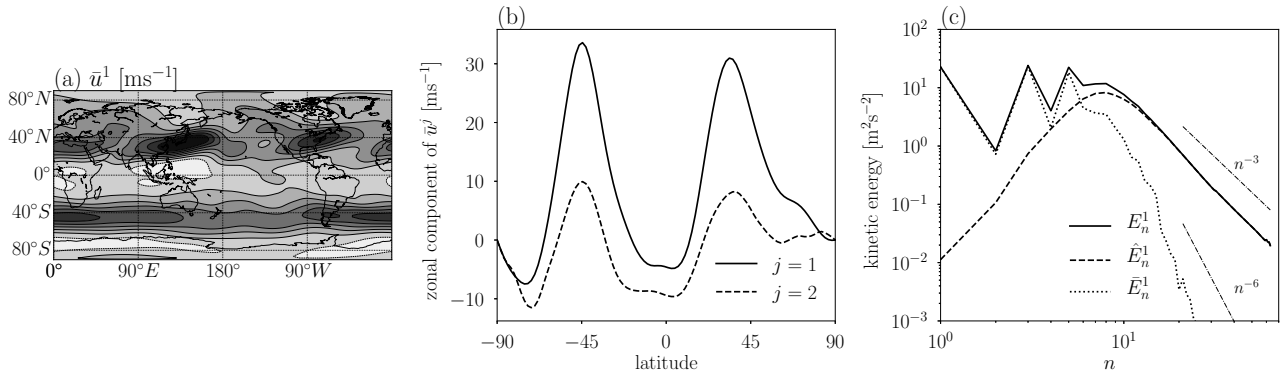

Figure 1: Flow characterisation: (a) zonal velocity field at level 1 with contour levels from -16 ms^{-1} (white) to 56 ms^{-1} (black); (b) zonal component of the time averaged zonal velocity at level 1 and 2; and (c) kinetic energy spectra (E_n^1) of the DNS decomposed into contributions from the mean field ($\bar{E}_n^1$) and fluctuating field ($\hat{E}_n^1$) at level 1.

with T the DNS truncation wavenumber. Note, all results are non-dimensional unless units are specified.

The present DNS has a truncation wavenumber of $T = 63$, corresponding to 192×96 grid points (in latitude $\times$ longitude), which is equivalent to a grid spacing in the mid-latitudes of approximately 100 km. Here $F_L = 2.5 \times 10^{-6}$ km^{-2}, which correspond to a Rossby radius of deformation of $r_{\text{Ros}} = 1/\sqrt{2F_L} =$ 447 km, of associated wavenumber $k_{\text{Ros}} = a/r_{\text{Ros}} = 14$. Baroclinic instability is, therefore, explicitly resolved since $T \gg k_{\text{Ros}}$. The interaction coefficients K_{nqs}^{mpr} are detailed in [5], and the Kroncker delta term δ^{j2} in (1) ensures that the spectral topography, h_{mn}, enters into the equations only for the lower level. The Rossby wave frequency is $\omega_{mn} = -2m/(n(n+1))$. The drag at each level is only applied to the large scales $n \leq 15$ and $m \leq 15$, with damping times ($1/\alpha_n^j$) of 20 days for level 1 and 5 days for level 2. The model is driven toward the mean January state, $\tilde{q}_{mn}^j$, for scales $n \leq 32$ and $m \leq 32$, with a relaxation time ($1/\kappa_n$) of 11.6 days. The isotropic bare dissipation $D_0^l(n)$ is set according to the self-similar scaling laws outlined in [6], such that the present benchmark DNS has statistics consistent with like simulations of arbitrary high horizontal resolution. In [6] the climate was only a function of the level and latitude. However, in the present work the climate state is fully three-dimensional.

The mean and fluctuating fields of this atmospheric flow are now characterised. The mean jets are characterised by their zonal velocity ($\bar{u}^j$), and illustrated for level $j = 1$ in figure 1(a). The easterly jets have similar strength in both hemispheres. They also exhibit zonal asymmetries as a result of the target fields and topography. The zonal component of the jets on both levels are illustrated in figure 1(b), with the lower level jets clearly weaker than the upper level ones. The contribution of the meanfield and transients to each scale are illustrated by the m-summed kinetic energy spectra. The January spectra at the top level are illustrated in figure 1(c). The meanfield kinetic energy ($\bar{E}_n^1$) dominates for the large scales (small wavenumbers), and the transient kinetic energy ($\hat{E}_n^1$) dominates at the small scales (large wavenumbers). The two components have equivalent magnitude at $n \approx 6$. A constant enstrophy flux inertial range starts at $n \approx 20$, at which point the transients are two orders of magnitude greater than the meanfield [6]. From $n = 20$ onwards, the kinetic energy spectra exhibits an n^{-3} decay, consistent with a constant enstrophy flux [6]. The meanfield spectra drops off far more quickly, and is closer to a n^{-6} dependence. The lower level has similar properties, but has a lower magnitude across practically all scales.

Stochastic subgrid parameterisation framework

Here we present a framework for determining the subgrid coefficients from the statistics of the DNS. The first step is to determine the subgrid tendency associated with a particular lower resolution LES truncation wavenumber T_R. The LES is confined to the resolved scale wavenumber set $\mathbf{R} \equiv \mathbf{T}(T_R)$. The subgrid wavenumber set is defined as $\mathbf{S} = \mathbf{T} - \mathbf{R}$. To facilitate the following discussion, we let $\mathbf{q} = (q_{mn}^1, q_{mn}^2)^T$ for a given wavenumber pair. In this vector notation the time derivative of $\mathbf{q}$ can be decomposed such that $\mathbf{q}_t(t) = \mathbf{q}_t^{\mathbf{R}}(t) + \mathbf{q}_t^{\mathbf{S}}(t)$. The resolved tendency ($\mathbf{q}_t^{\mathbf{R}}$) involves only triadic interactions between wavenumbers less than or equal to T_R, whilst the subgrid tendency ($\mathbf{q}_t^{\mathbf{S}}$) has at least one wavenumber greater than T_R involved in the triadic interactions. The subgrid tendency is further decomposed as $\mathbf{q}_t^{\mathbf{S}}(t) = \bar{\mathbf{f}} + \hat{\mathbf{q}}_t^{\mathbf{S}}(t)$ where $\bar{\mathbf{f}}$ is its time average representing the sum of the E-M, M-M, and E-T interactions, and $\hat{\mathbf{q}}_t^{\mathbf{S}}$ is its fluctuating component representative of the E-E interactions.

We adopt the approach of [5] to parameterise $\hat{\mathbf{q}}_t^{\mathbf{S}}$ through

$$\hat{\mathbf{q}}_t^{\mathbf{S}}(t) = -\mathbf{D_d}\ \hat{\mathbf{q}}(t) + \hat{\mathbf{f}}(t)\ , \tag{3}$$

where $\mathbf{D_d}$ is the subgrid drain dissipation matrix, $\hat{\mathbf{q}}$ is the fluctuating component of $\mathbf{q}$, and $\hat{\mathbf{f}}$ is a random forcing vector. As the present simulations have two vertical levels, $\mathbf{D_d}$ is a 2×2 matrix, and $\hat{\mathbf{f}}$ is a 2 element column vector. We determine $\mathbf{D_d}$ by post-multiplying both sides of (3) by $\hat{\mathbf{q}}^\dagger(t_0)$, integrating over the turbulent decorrelation period τ, and ensemble averaging, to yield

$$\mathbf{D_d} = -\left\langle \int_{t_0}^{t} \hat{\mathbf{q}}_t^{\mathbf{S}}(\sigma)\hat{\mathbf{q}}^\dagger(t_0)d\sigma \right\rangle \left\langle \int_{t_0}^{t} \hat{\mathbf{q}}(\sigma)\hat{\mathbf{q}}^\dagger(t_0)d\sigma \right\rangle^{-1}, \tag{4}$$

where $\dagger$ denotes the Hermitian conjugate for vectors and matrices. The angled brackets denote ensemble averaging, with each ensemble member determined by shifting the initial time t_0 and the final time $t = t_0 + \tau$ forward by one time step. The turbulence decorrelation time, $\tau = 192$ days, which is sufficiently large to capture the memory effects of the subgrid turbulence [6]. The model for $\hat{\mathbf{f}}$ is determined by calculating the non-linear noise covariance matrix $\mathcal{F}_b = \mathbf{F_b} + \mathbf{F_b}^\dagger$, where $\mathbf{F_b} = \langle \hat{\mathbf{f}}(t)\ \hat{\mathbf{q}}^\dagger(t) \rangle$. Again post-multiplying both sides of (3) by $\hat{\mathbf{q}}^\dagger(t)$, and adding the conjugate transpose of (3) pre-multiplied by $\hat{\mathbf{q}}(t)$ yields

$$\begin{aligned} \left\langle \hat{\mathbf{q}}_t^{\mathbf{S}}(t)\hat{\mathbf{q}}^\dagger(t) \right\rangle \quad &+ \quad \left\langle \hat{\mathbf{q}}(t)\hat{\mathbf{q}}_t^{\mathbf{S}\dagger}(t) \right\rangle = \\ -\mathbf{D_d}\left\langle \hat{\mathbf{q}}(t)\hat{\mathbf{q}}^\dagger(t) \right\rangle \quad &- \quad \left\langle \hat{\mathbf{q}}(t)\hat{\mathbf{q}}^\dagger(t) \right\rangle \mathbf{D_d}^\dagger + \mathcal{F}_b\ , \end{aligned} \tag{5}$$

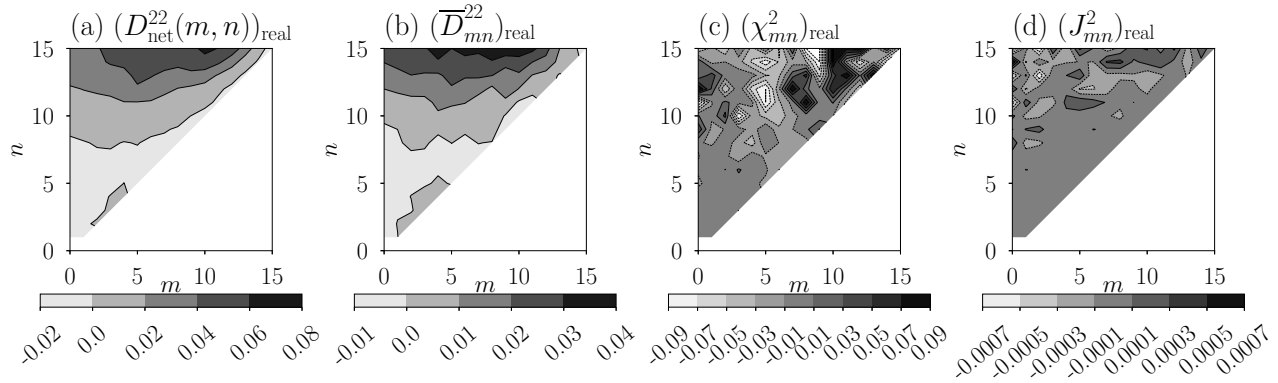

Figure 2: Subgrid coefficients: (a) eddy-eddy net dissipation $D^{22}_{\rm net}(m,n)$; (b) eddy-meanfield dissipation $\bar{D}^{22}_{mn}$; and (c) eddy-topographic term χ^2_{mn}; and (d) meanfield jacobian J^2_{mn}.

which can be rearranged for $\mathcal{F}_b$. An eigenvalue decomposition of $\mathcal{F}_b$ is used to produce a stochastic representation for $\hat{\mathbf{f}}$ [10]. The backscatter dissipation is then given by $\mathbf{D_b} = -\mathbf{F_b}\left\langle \hat{\mathbf{q}}(t)\,\hat{\mathbf{q}}^\dagger(t)\right\rangle^{-1}$. One can also represent the subgrid interactions in a simplified deterministic form $\hat{\mathbf{q}}^{\mathbf{S}}_i(t) = -\mathbf{D_{net}}\,\hat{\mathbf{q}}(t)$ where $\mathbf{D_{net}}$ is given by the sum of the drain and backscatter, representing the net effect.

The subgrid E-M, M-M and E-T interactions, all contribute to the mean subgrid tendency. A new least squares approach is developed to decompose their contributions, which makes use of the functional forms of the above subgrid terms outlined in the QDIA closure [3]. It captures the relationship that the ensemble averaged subgrid tendency $\bar{\mathbf{f}}$ has with the ensemble averaged field $\bar{\mathbf{q}}$, and the topography h_{mn}. For a given wavenumber pair

$$\bar{\mathbf{f}} = -\overline{\mathbf{D}}\bar{\mathbf{q}} + \chi h_{mn} + \mathbf{J}\,, \tag{6}$$

where $\overline{\mathbf{D}}$ is a 2×2 dissipation matrix representing the E-M interactions, the E-T term χ is a 2 element column vector, and the meanfield Jacobian $\mathbf{J}$ is a time invariant 2 element vector given by

$$J^j_{mn} = \sum_{(p,q,r,s)\in\mathbf{S}} \mathrm{i}K^{mpr}_{nqs}\left(\langle\bar{\psi}^j_{-pq}\rangle\langle\bar{q}^j_{-rs}\rangle + \langle\bar{\psi}^j_{-pq}\rangle h_{-rs}\delta^{j2}\right)\,. \tag{7}$$

The matrix $\bar{\mathbf{D}}$ is then solved for in a least squares sense,

$$\bar{\mathbf{D}} = -\left(\langle(\bar{\mathbf{f}}_i - \mathbf{J}_i)\bar{\mathbf{q}}_i^\dagger\rangle - (\bar{\mathbf{f}}-\mathbf{J})\bar{\mathbf{q}}^\dagger\right)\left(\langle\bar{\mathbf{q}}_i\bar{\mathbf{q}}_i^\dagger\rangle - \bar{\mathbf{q}}\bar{\mathbf{q}}^\dagger\right)^{-1}\,, \tag{8}$$

where $\bar{\mathbf{q}}_i$ and $\bar{\mathbf{f}}_i$ are time averaged over the i-th non-overlapping time window of length τ_M, and $\mathbf{J}_i$ is calculated from $\mathbf{q}_i$. By definition the ensemble averages $\langle\mathbf{q}_i\rangle \equiv \bar{\mathbf{q}}$, and $\langle\bar{\mathbf{f}}_i\rangle \equiv \bar{\mathbf{f}}$. The topography h and E-T coefficient χ are both independent of time and hence ensemble member. We use $\tau_M = 32$ days, since the magnitude of the subgrid coefficients at the truncation scale are practically independent of τ_M for longer periods. The E-T term is then determined by rearranging (6) such that

$$\chi \quad = \quad \left[\bar{\mathbf{f}} + \overline{\mathbf{D}}\bar{\mathbf{q}} - \mathbf{J}\right]/h_{mn}\,. \tag{9}$$

Subgrid coefficients

As discussed above the deterministic variant of the E-E interactions are parameterised via a net dissipation matrix $\mathbf{D_{net}}$ acting upon the fluctuating field. At the truncation level of $T_R = 15$ baroclinic instability (of central wavenumber $k = 14$) is not explicitly resolved, and the associated energy injection into the system must be parameterised. The real component of the upper diagonal element of $\mathbf{D_{net}}$ is illustrated in figure 2(a). The dissipation increases strongly with n indicating that the E-E subgrid interactions become stronger as the resolved scales approach the truncation wavenumber. The positive dissipations for large n indicate energy being deterministically transferred from the resolved to the subgrid, whilst negative values for small n indicate an energy being transferred from the subgrid to the resolved scales.

The mean subgrid tendency ($\bar{\mathbf{f}}$) is decomposed into the: E-M ($-\bar{\mathbf{D}}\bar{\mathbf{q}}$); E-T ($\chi h_{mn}$); and M-M ($\mathbf{J}$) components. The real components of $\bar{D}^{22}_{mn}$, χ^2_{mn} and J^2_{mn}, are respectively illustrated in figure 2(b), 2(c) and 2(d). The upper diagonal E-M dissipation ($\bar{D}^{22}_{mn}$), is either zero or negative through most of the wavenumber plane, with positive values in the region approaching the truncation scale. This indicates that the large scale mean climate state needs to be energised due to the unresolved baroclinic instability. The magnitudes of the other coefficients also increase with n, however, they also change sign often in both the n and m directions. The above observations are also true for level $j = 1$.

Large eddy simulation

The relative impact of each of the subgrid interactions upon the kinetic energy spectra is illustrated in figure 3(a). As a baseline the first test is the no subgrid parameterisation case ($\mathbf{q}^{\mathbf{S}}_i = 0$). This obviously produces ridiculous results with a build up of energy in the smallest resolved scales. It also clearly illustrates a decrease in energy at the large scales, as a result of the *"tail wagging the dog"* effect of [4]. This is due to the dynamical system attempting to globally conserve energy to counter the build up of energy at the small scales.

Each of the following tests all adopt the determinisitic E-E parameterisation, where for a given (m,n) wavenumber pair the fluctuating subgrid tendency is parameterised according to $-\mathbf{D_{net}}\hat{\mathbf{q}}$. The second test is the no subgrid meanfield tendency ($\bar{\mathbf{f}} = 0$). As can be seen the addition of the E-E model has largely corrected the spectra. The following tests progressively include the E-M component ($\bar{\mathbf{f}} = -\bar{\mathbf{D}}\bar{\mathbf{q}}$); the E-T components ($\bar{\mathbf{f}} = -\bar{\mathbf{D}}\bar{\mathbf{q}} + \chi h_{mn}$); and finally the meanfield Jacobian ($\bar{\mathbf{f}} = -\bar{\mathbf{D}}\bar{\mathbf{q}} + \chi h_{mn} + \mathbf{J}$). As one would expect, the bottom spectra incorporating all of the subgrid interactions yields the best agreement. Each of these LES variants are also compared on the basis of the zonal component of the mean zonal velocity at level 1 in figure 3(b). By this measure the E-E parameterisation is again responsible for the greatest improvement, but the best agreement is achieved when all interactions are parame-

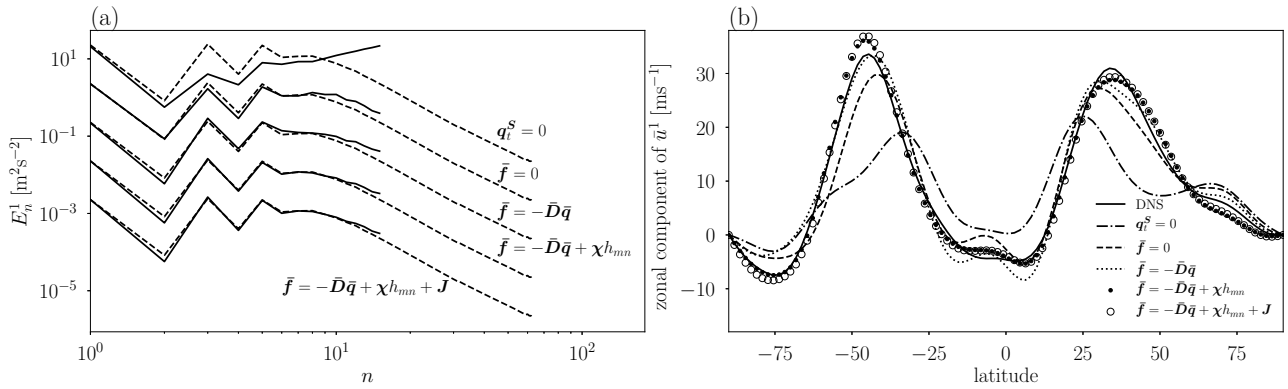

Figure 3: LES validation. (a) Comparison of the level 1 kinetic energy spectra between the DNS (dashed line) to LES variants (solid line) with no subgrid parameterisation ($\mathbf{q}_l^{\mathbf{S}} = 0$), only the deterministic E-E parameterisation ($\bar{\mathbf{f}} = 0$), plus the E-M component ($\bar{\mathbf{f}} = -\bar{\mathbf{D}}\bar{\mathbf{q}}$), plus the E-T component ($\bar{\mathbf{f}} = -\bar{\mathbf{D}}\bar{\mathbf{q}} + \chi h_{mn}$), and finally the complete subgrid parameterisation ($\bar{\mathbf{f}} = -\bar{\mathbf{D}}\bar{\mathbf{q}} + \chi h_{mn} + \mathbf{J}$). The top spectra is at the true energy level with the others offset for clarity. (b) Comparison of the above variants on the basis of the zonal component of $\bar{u}^1$.

terised. Note, equally impressive agreement is achieved using the stochastic E-E parameterisation.

Concluding remarks

We have presented a framework for how one can parameterise each of the dominant subgrid interactions, from the statistics of a benchmark DNS. The E-E interactions are between subgrid eddies and resolved eddies, and are the dominant class. In the present LES they are parameterised via a scale dependent dissipation acting on the resolved transient field. The E-M interactions are between the subgrid eddies and the resolved meanfield, and are parameterised as being linearly proportional to the resolved meanfield. The E-T interactions are those between the subgrid eddies and the resolved topography and is linearly proportional to the latter. The M-M interactions are those between the resolved meanfield and resolved topography, and the subgrid meanfield and subgrid topography. Successful LES are presented for a truncation in which baroclinic instability is not fully resolved ($T_R = 15$) using 1.3% of the computational effort used in the DNS. Whilst the E-E interactions are dominant, the best agreement between the LES and DNS is achieved when all of the subgrid interactions are parametrised. Our subgrid parameterisation are hence able to produce lower resolution simulations that reproduce the statistics of a higher resolution reference case across all scales. The framework outlined herein is not specific to the atmosphere, nor canonical fluid dynamics. In fact it is a general means of parametrising unresolved processes in nonlinear multi-scale inhomogeneous dynamical systems.

Acknowledgements

We acknowledge Meelis J. Zidikheri for providing the relaxation climate states, and the NCI for the computational resources. V. Kitsios was supported by the Australian CSIRO Decadal Forecasting Project (research.csiro.au/dfp).

References

[1] Frederiksen, J. S., Precursors to blocking anomalies: the tangent linear and inverse problems, *J. Atmos. Sci.*, **55**, 1998, 2419–2436.

[2] Frederiksen, J. S., Subgrid-scale parameterizations of eddy-topographic force, eddy viscosity and stochastic backscatter for flow over topography, *J. Atmos. Sci*, **56**, 1999, 1481–1493.

[3] Frederiksen, J. S., Statistical dynamical closures and subgrid modeling for inhomogeneous QG and 3D turbulence, *Entropy*, **14**, 2012, 32–57.

[4] Frederiksen, J. S., Dix, M. R. and Kepert, S. M., Systematic energy errors and tendency toward cannonical equilibrium in atmospheric circulation models, *J. Atmos. Sci.*, **53**, 1996, 887–904.

[5] Frederiksen, J. S. and Kepert, S. M., Dynamical subgrid-scale parameterizations from direct numerical simulations, *J. Atmos. Sci.*, **63**, 2006, 3006–3019.

[6] Kitsios, V., Frederiksen, J. S. and Zidikheri, M. J., Subgrid model with scaling laws for atmospheric simulations, *J. Atmos. Sci.*, **69**, 2012, 1427–1445.

[7] Kitsios, V., Frederiksen, J. S. and Zidikheri, M. J., Scaling laws for parameterisations of subgrid eddy-eddy interactions in simulations of oceanic circulations, *Ocean Model.*, **68**, 2013, 88–105.

[8] Kitsios, V., Sillero, J. A., Frederiksen, J. S. and Soria, J., Scale and Reynolds number dependence of stochastic subgrid energy transfer in turbulent channel flow, *Comp. Fluids*, **151**, 2017, 132–143.

[9] O'Kane, T. J. and Frederiksen, J. S., Statistical dynamical subgrid-scale parameterizations for geophysical flows, *Phys. Scr.*, **T132**, 2008, 014033 (11pp).

[10] Zidikheri, M. J. and Frederiksen, J. S., Stochastic subgrid parameterizations for simulations of atmospheric baroclinic flows, *J. Atmos. Sci.*, **66**, 2009, 2844–2858.

[11] Zidikheri, M. J. and Frederiksen, J. S., Stochastic subgrid-scale modelling for non-equilibrium geophysical flows, *Phil. T. Roy. Soc. A*, **368**, 2010, 145–160.